HETEROSTRUCTURE TYPE TRANSFORMATION OF TERNARY ZnTe$_x$Se$_{1-x}$/ZnSe CORE/SHELL QUANTUM DOTS

GUOZHI JIA[*], YUNFENG WANG[a], LEI GONG, JIANGHONG YAO
Tianjin Institute of Urban Construction, Tianjin 300384, China
[a]The Key Laboratory of Advanced Technique and Fabrication for Weak-Light
Nonlinear Photonics Materials, Ministry of Education, Nankai University, Tianjin
300457, China

The electronic structures of ZnTe$_x$Se$_{1-x}$/ZnSe core/shell structure QDs have been investigated by effective-mass approximation method with taking into the Coulomb interaction account. The heterostructure type of QDs can be tuned from the type-I to type-II by changing the Se molar fraction in the core layer and the corresponding "spatially indirect" energy gap formed. We demonstrate that the bowing parameter in the ternary core is key to the transformation from the type-I to type- II. The transition energies can be widely tuned by the changing the Se molar fraction in the core layer and core radius.

1. Introduction

Colloidal core/shell semiconductor quantum dots (QDs) are typically classified as type-I and type-II by combining different materials with the relative alignment of conduction and valence band edges at the heterointerface of QDs. [1-5] In the type-I QDs structure, both an electron and a hole reside in the core part of QDs due to the conduction and the valence band edges of the core located within the energy gap of the shell. Contrary to type-I, type-II structure QDs alignment spatially separate carriers into the two different range of the core and shell due to the lowest energy states for electrons and holes in the different layer of QDs. This can be engineered to emit longer wavelength than one of either semiconductor comprising QDs.[2,4] The effective band gaps of type-II structure QDs is smaller than the energy gap of the core and shell materials and mainly determined by the band offsets and size of the core and shell.[2,4,9] Additionally, the Auger and radiative decay lifetime can be slowed due to the excitons separated in the different areas of the type-II structure QDs.[10] The carriers spatial separation of the type-II structure QDs provides new means of controllable wavefunction and makes these structures QDs be beneficial for photovoltaic or photoconduction applications. [2,4,6]

A great deal of work on the type-II heterostructure nanocrystals has been mainly focused on the binary semiconductor compounds by various preparing techniques.[2-7.,9, 11-18]. To date, a type-I to type-II band alignment transition is reported by varying the InAsSb composition from

---

pure InAs to InSb, which develop a means to tailoring the band structure. [19] The ternary core/shell structures offer a new way to tuning the optical and electrical properties of QDs by not only the dimensions, shape, and sizes, but also the composition. The QDs with a ternary semiconductor compound core can produce a new degree of freedom for tailoring the band structure. Therefore, it is essential to analyze the quantum confinement in the ternary QDs structure to understand the physics for developing the QDs performance. In addition, ternary semiconductor QDs with both homogeneous and gradient composition have been fabricated via pyrolysis of organometallic precursors.[20] Zhong *et al.* prepared the high-quality $Zn_xCd_{1-x}Se$ nanocrystals at high temperature by incorporating stoichiometric amounts of Zn and Se into preprepared CdSe nanocrystals. Wang *et al.* [21] synthesized $Zn_xCd_{1-x}Te$ alloyed nanocrystals with different compositions in aqueous solution with thioglycolic acid as stabilizer [22]..Ternary semiconductor compounds provides greater tuning range of lattice constant and energy levels than the binary compounds. The energy levels of ternary semiconductor compounds can easily be changed by controlling the composition ratio. The knowledge of the electronic structure properties is the key to expand ternary semiconductor compounds in the application of core-shell structure. In particular, composition-dependent optical and electronic properties of the ternary core/shell QDs were few reported. In addition, Cd-free QDs were proved their potentials toward "nontoxic" biological or medical applications that are free from concerns regarding heavy-metal leakage [6]. Thus, it also is essential to expand the degree of freedom for tuning the optical characterize by heterostructure type and multiple component compoud.

Currently, more theoretical study have showed the effective mass approximation (EMA) is an important method to theoretically research the quantum confinement effect, and can be applied to the core/shell QDs to quantify the energy levels.[2,3,10,23] The EMA can be applied to calculate the electronic structure of the core/shell QDs, the electron and hole wave functions, the transition energy, and the overlap of the wave functions. Sergei *et al.* performed a theoretical modeling of the core/shell nanocrystals using effective mass approximation and applying first-order perturbation theory, and determine the range of geometrical parameters of the core/shell structures that result in a type-II localization regime. [2]. Haus *et al.* applied the effective mass approximation to calculate the electronic structure of Quantum-dot quantum well (QDQW). They systematically investigated the electron and hole wave functions, the 1*s* transition energy, and the overlap of the wave functions[5]. Schooss *et al.* further take into account the Coulomb interaction between electron and hole, the results showed that the probabilities of the carriers can present in the different layers in the QDQW CdS/HgS/CdS structure [24]. Chang *et al.* pointed out that the spatially separated characteristic of electron and hole can be enhanced significantly in QDQW with the two wells [25]. More recently, Nizamoglu *et al.* presented that the multi-color spontaneous emission can be obtained by the exciton localization in distinct layers in the onion-like QDQW structure [23] It is therefore of great interest and importance to engineer spatial distributions wave function of electron and hole in nano-particles.

In this paper, we present a type-I to type-II band alignment transition by varying the Se molar composition in the ternary semiconductor core/shell structure QDs. The simple EMA model was used to study the electron structure, band energy, and overlap intergral in $ZnTe_xSe_{1-x}/ZnSe$ core/shell QDs with taking into the Coulomb interaction account. The electron and hole wave function behaviors in $ZnTe_xSe_{1-x}/ZnSe$ core/shell structure nanocrystals were investigated with the changing of the structure parameters and the component ratio of $ZnTe_xSe_{1-x}$. The electron and hole

wave functions, the 1s transition energy, and the overlap of the wave functions is analyzed. The transition mechanism between type-I and type-II is discussed, in which the main reason is attributed to the blending of the velence band at the heterostructure interface between the ternary material ZnTe$_x$Se$_{1-x}$ core and ZnSe shell.

2. Theory

We consider the core/shell structure QDs, which consisted of ZnS shell and CdS core materials. When the space-dependent effective mass of carriers is taken into account, the Schrodinger equation of carriers in the framework of the single-band effective mass approximation in the QDs region is as follows:

$$\left(-\frac{\hbar^2}{2}\nabla\frac{1}{m_i}\nabla - V\left(r\right) \right)\Psi(r) = E\Psi(r) \tag{1}$$

where $\hbar$ is Planck's constant divided by 2π, m_i and $V(r)$ the particle mass and a potential depending on the position in the QDs, E the energy eigenvalue, and $\psi(r)$ the corresponding eigenfunction. Here, we consider QDs with spherically symmetric structure and homogeneous potentials, which leads to separate the wave functions into the radial and angular parts as follows:

$$\Psi_{nlm}(r,\theta,\phi) = R_{nl}(r)Y_{lm}(\theta,\phi) \tag{2}$$

$R_{nl}(r)$ is the radial wave function, and $Y_{lm}(\theta,\phi)$ a spherical harmonic. n is the principal quantum number, and l and m are the angular momentum numbers. We shall restrict the calculations to 1s states for $n=1$, $l=m=0$. We obtain the solutions for QDs by solving the continuity relations of the carriers wave functions and the probability currents at the boundaries:

$$R_{nl,i}(k_i r_i) = R_{nl,i+1}(k_{i+1}r_i) \tag{3}$$

$$\frac{1}{m_i}\frac{dR_{nl,i}(k_i r_i)}{dr}\bigg|_{r=r_i} = \frac{1}{m_{i+1}}\frac{dR_{nl,i+1}(k_{i+1}r_i)}{dr}\bigg|_{r=r_i} \tag{4}$$

where $k_{i/i+1} = \left[\dfrac{2m_i(E-V)}{\hbar^2}\right]^{1/2}$ is the wave vectors in core and shell, repectively, $R_{nl,i}(r_i)$ and $R_{nl,i+1}(r_i)$ are the radial wave functions for the carriers (electron or hole) in the core and shell, respectively, m_i and m_{i+1} are the carrier effective masses in the CdS and ZnS, respectively. For simplicity, we assume that the QDs are placed in a infinite potential well. That is to say, no wave functions tunnel from the QDs to the outside of QDs with taking into account the complete

confinement. Thus, at the outer boundary of the QDs, the nontrivial solution can be obtained to determine the general energy eigenvalues by letting the determinant of the coefficients of the wavefunction at the interface as zero.

The Coulomb interaction energy between electron and hole pair can be treated as a heliumlike perturbation according to the first-order perturbation approximation. After expanding of $1/|r_e - r_h|$ in spherical harmonics form and integrating the angular coordinates, the Coulomb interaction energy can be expressed as[23, 24]

$$E_c = -\frac{e^2}{4\pi\varepsilon_0} \iint dr_e dr_h r_e^2 r_h^2 \frac{|R_e(r_e)|^2 |R_h(r_h)|^2}{\max(r_e, r_h)\overline{\varepsilon}(r_e, r_h)} \tag{5}$$

For ternary semiconductor compound, the optical band-gap was given using bowing parameters:

$$E_g = xE_{gap}^{AB} + (1-x)E_{gap}^{AC} - b_{bow}x(1-x)$$

$$(6)$$

where E_{ZnTe} and E_{ZnSe} are the band gaps of binary compounds ZnTe and ZnSe, respectively, and b_{bowing} the bowing parameter, 1.647. [26] Tit *et al*. studied the origins of bandgap bowing in coumpound-semiconductor common-cation ternary alloys based on the sp^{3}s* tight-binding method, and show that the mismatch in electro-negativity between Te atom and Se atom would play a role in the bandgap bowing of alloys [27]. This can result in the velence band states lowing in energy with the increasing of Se molar fraction in the ternary alloy, while the cation Zn are contributors to the conduction band of the alloy. Here, it can be a very reasonable conjecture as follows: the conduction band edge was approximated by linear interpolation between that the constituent binary compounds, then the valence band edge was calculated by $E_V = E_C - E_g$. As far as the core/shell structure QDs is concerned, the strain plays a key role in the transition energy levels. The lattice parameter of ZnTe (a=6.104Å) is very close to the lattice parameter of ZnSe (a=5.669Å), which can be expected to exhibit well core/shell growth due to the small lattice mismatch. The lattice-mismatch between core and shell can further decrease with Se molar fraction increasing in the ternary alloy core.

3. Results and discussion

The schematic energy diagram of a ternary ZnTe$_{1-x}$Se$_x$/ZnSe core/shell QD under investigation is shown in Fig.1. The conduction band edge of ZnSe is taken as the energy reference (i.e. E_v=0). From the diagram, it can be inferred that ZnSe has the higher valence and conduction bands than ZnTe$_{1-x}$Se$_x$, as Se molar fraction x is lower than the band alignment transition point (about x=0.5), which corresponds to the classic Type-II semiconductor heterostructure. It is clearly seen that the valence band of ZnTe$_{1-x}$Se$_x$ bends and reduces to below the valence band bottom ZnSe as the increasing of Se molar fraction in the ternary ZnTe$_{1-x}$Se$_x$ core (0.5<x<1). The corresponding Type-I band alignment was formed, where both electron and hole were localized in

the core range. When the Se molar fraction change from 0 to 0.8, the conduction band offset changes from 1.060 eV to 0.212, the valence band offset from 0.530eV to -0.387. The transition point between Type-I and Type-II is heavily governed by quantum confinement effect. According to the conduction (valence) band energy alignment between the ternary $ZnTe_{1-x}Se_x$ core and the ZnSe shell, the heterostructure types of QDs can be classified as Type-I, quasi Type-II, and Type-II with changing of the Se molar composition in QDs. As for quasi Type-II of the $ZnTe_{1-x}Se_x$/ZnSe core/shell QDs, the electron is confined to the shell region while the hole is distributed in the entire volume of QDs[2], which corresponds to partial charge separation.
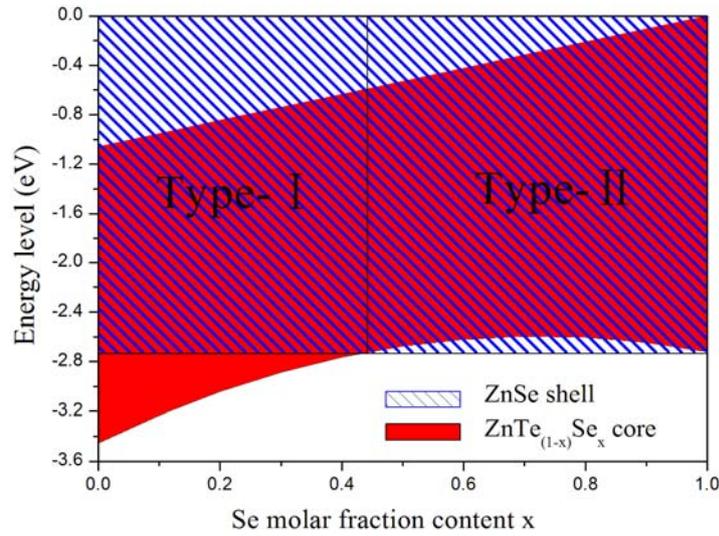
Fig. 1 Band-edge alignments at the heterointerface between the ternary ZnTeSe core and ZnSe shell. In the Type-II structure, the electron and hole are spatially separated in the core and shell region, respectively. In the Type-I structure, the carriers are localized in the same region.

In the following, we present the numerical results for the ternary $ZnTe_{1-x}Se_x$/ZnSe core/shell QDs. The material parameters used in calculation are listed in Table 1. Fig. 2 shows the variation of the energies of electron and hole levels in the ternary $ZnTe_{1-x}Se_x$/ZnSe core/shell QDs as a function of the core radius for different Se molar fraction, i.e., x=0, 0.2, 0.4, 0.6, and 0.8, respectively. From Fig. 2 we find that the dependence of energies of electron level on core radius is more obvious than those of the hole level. It is readily seen that the changing of the electron energies level of strong-confinement QDs (with small core radius) is much larger than that of weak-confinement QDs (with large core radius) in the same Se molar fractions. The carriers should appear in the region of core or shell, which mainly depend on the competition between the kinetic energy and the potential energy in the heterostrucuture QDs. [5] The shift of the lowest energy state results from the large energy levels offset for the fixed QDs size. As the Se molar composition in the ternary core of QDs is fixed, the changing of the lowest energy level can be ascribed to the variation of QDs size.

Table 1. Material parameters for ZnTe and ZnSe

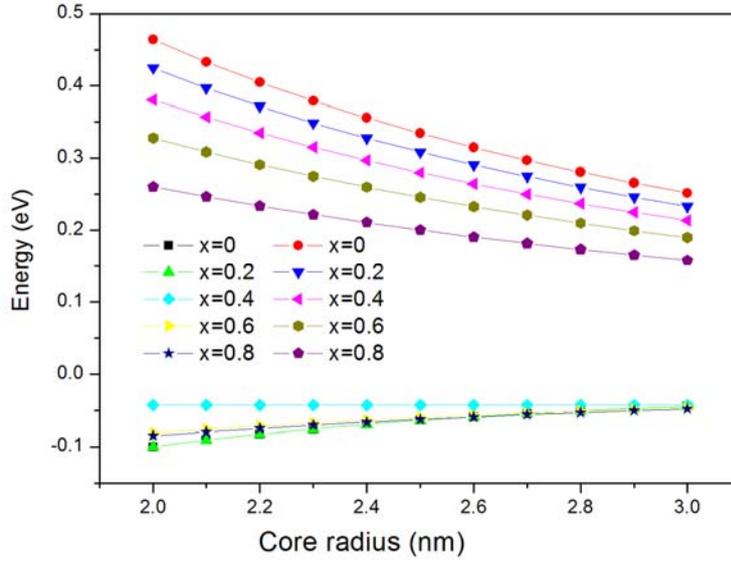| Material	m_e/m_0	m_h/m_0	Dielectric constants	Band gap (eV)
ZnTe	0.11[28]	0.7[29]	7.78	2.39
ZnSe[2]	0.14	0.6	8.1	2.72

Fig. 2 The energies of the electron and hole in the lowest energy 1s eigenstates as a function of the core radius in ZnTeSe/ZnSe QDs structure with the different Se molar fraction.

In order to study the effect of Se molar fraction in the ternary $ZnTe_{1-x}Se_x$ core on the spatial distribution of carriers, we analyze the overlap integral between electron and hole functions defined as $\Theta = \left| \int_0^{R+H} r^2 \mathfrak{R}^e(r)\mathfrak{R}^h(r)dr \right|^2$, where r is the radial coordinate with the origin at the core center and $\mathfrak{R}^{e(h)}(r)$ is the radial part of the electron (hole) envelope wavefunction. Fig. 3 shows the overlap integral for fixed values of the shell thickness ($H = 2nm$) as a function of the core radius for the different Se molar fraction in the ternary $ZnTe_{1-x}Se_x$ core. An interesting finding is that the overlap integral exhibit a transformation from type-I to type-II. For Se molar fraction in the ternary $ZnTe_{1-x}Se_x$ core less than 0.2, the results indicate that the type-II localization of carries, which correspond to the "spatially indirect" energy gap. When x is larger than 0.6, the overlap integral is close to unity and keep constant with the increasing of core radius. It can also been seen that the overlap integral can reduce with increasing of the core radius for the small Se molar
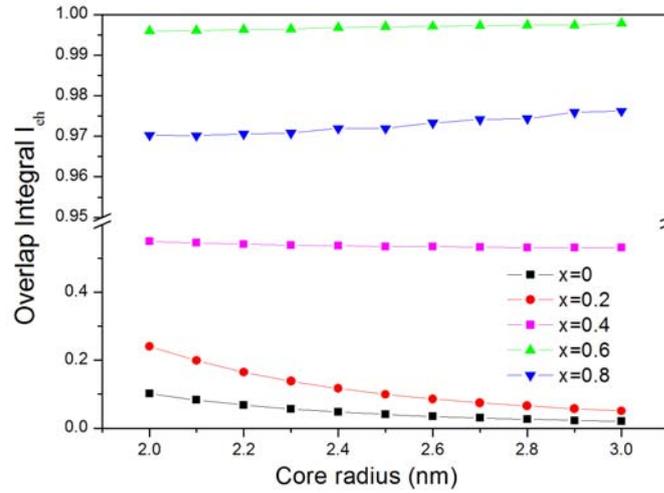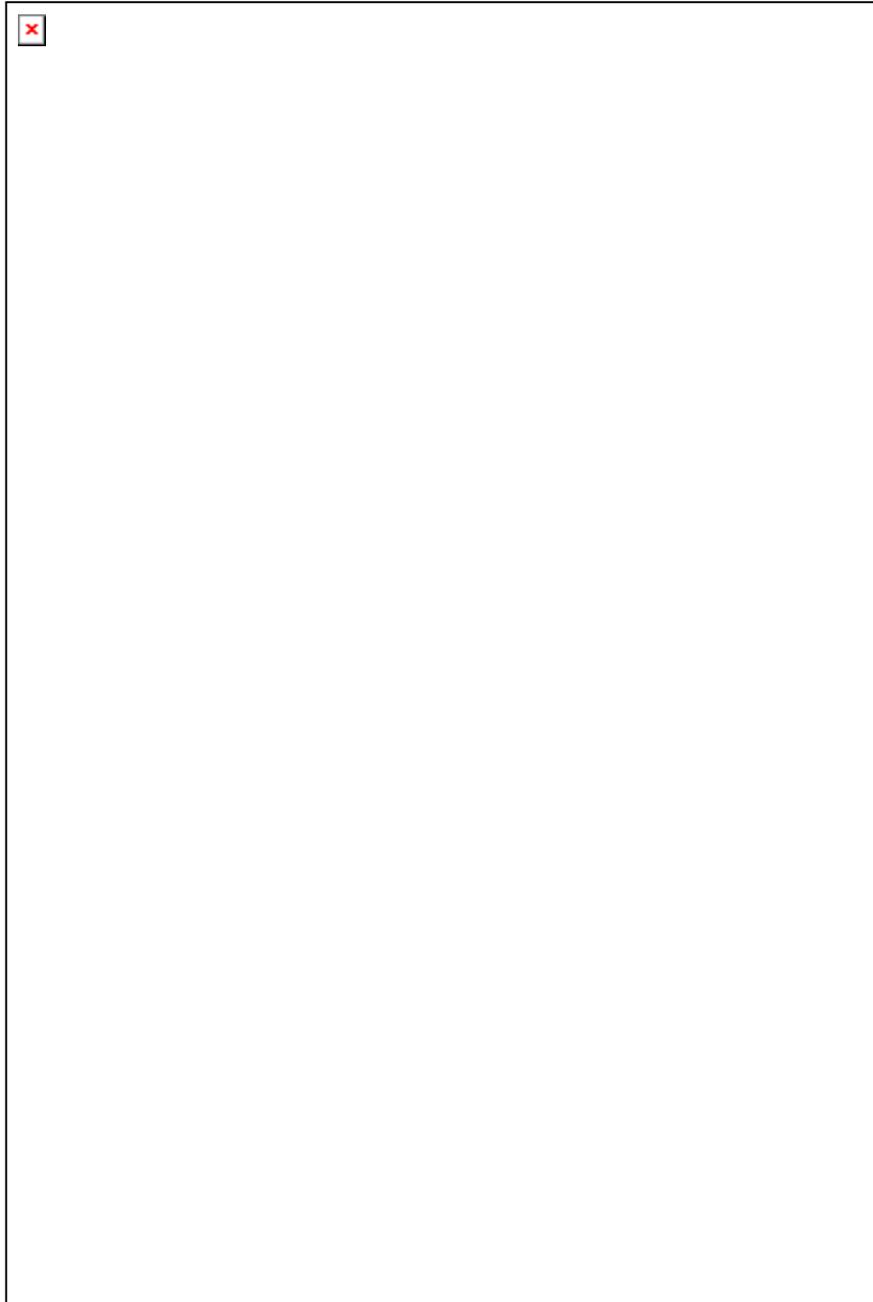
fraction.

Fig. 3 The calculation of the overlap integral as a function of the core radius with the different Se molar fraction in ZnTeSe/ZnSe QDs for the shell size fixed ($r = 3nm$).

To further understand the separation of electrons and holes in the ternary core/shell QDs, we shows the behavior of the wavefunction of electron and hole for fixed values of the core radius and shell thickness as a function of Se molar fraction in the core. From the Fig.4, it can be seen that the carrier distribution can be tunned from type-I to type-II by changing the Se molar fraction in the $ZnTe_{1-x}Se_x$ core. The electron wavefunction has a little change in the QDs with the changing of Se molar fraction, and mainly reside in the range between 1nm to 3nm. It can be found that the distribution maxima of the electron didn't localized in the core, even though the conduction band edge of the core is lower than that of the shell, the quantum confinement effect can play an important role in the distribution of electron, especially, for the core with only 3 nm radius. As the Se molar fraction changes from the 0 to 0.4, the holes primarily reside in the shell layer. The overlapping between electron and hole wavefunctions is very small, showing nearly complete spatial separation between electron and hole. The charge carriers are confined to the same range with the increasing of Se molar fraction, indicating the type-I carrier localization.

Fig. 4 The probability of the presence of electron and holes in the lowest energy 1s eigenstates in ZnTeSe/ZnSe QDs structure with the different Se molar fraction in the ternary semiconductor core and keeping the core radius and shell size constant $r = 3nm$, $H = 2nm$.

Fig.5 shows the band gap energy of the ground state for the ternary $ZnTe_{1-x}Se_x$/ZnSe core/shell as a function of the core radius for the five different Se molar fraction x=0, 0.2, 0.4, 0.6, and 0.8, respectively. From the figure, it can be clearly seen that the band edge transition energy in the structure with low Se molar fraction (for example, x=0, and 0.2) is smaller than the energy gap of either ZnTe (2.39eV) or ZnSe (2.72eV), which further indicates the type-II structure formed between the core and shell. As the Se molar fraction is larger 0.6, the transition energy is larger than the band gap energy of the ternary $ZnTe_{1-x}Se_x$ core with the same Se molar fraction, transforming into the type-I structure QDs. This shows that the Se molar fraction in the ternary

ZnTe$_{1-x}$Se$_x$ core is the critical determinant of the QDs energy levels. The changing of molar fraction in the ternary ZnTe$_{1-x}$Se$_x$ core results in the variation of the effective masses of electron and hole, and the band offset between the core and shell changed. In addition, the valence band bows in the ternary semiconductor compound can be main factor of the transition from type-I to type-II structure.
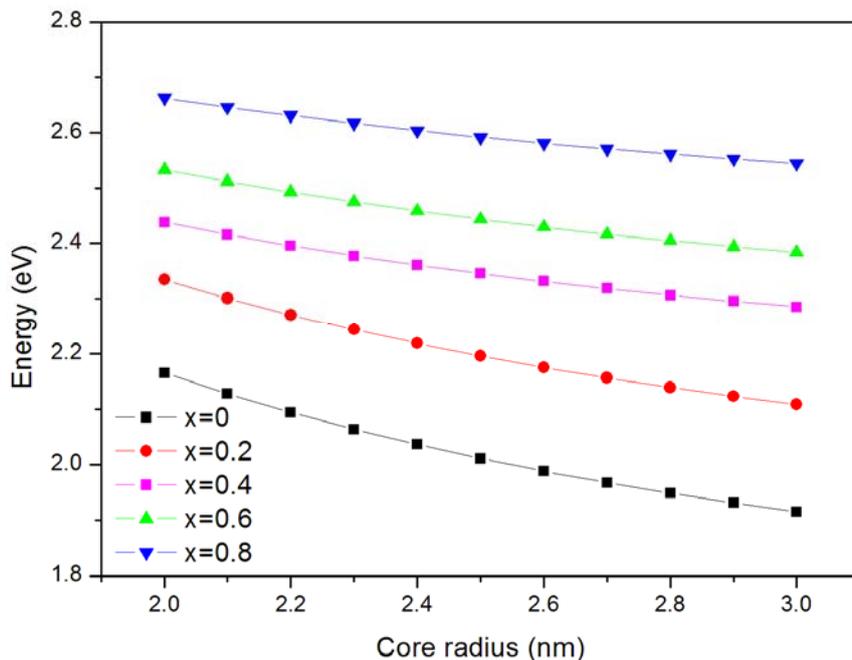

Fig. 5 The lowest energy 1s eigenstates as a function of the core radius in ZnTeSe/ZnSe
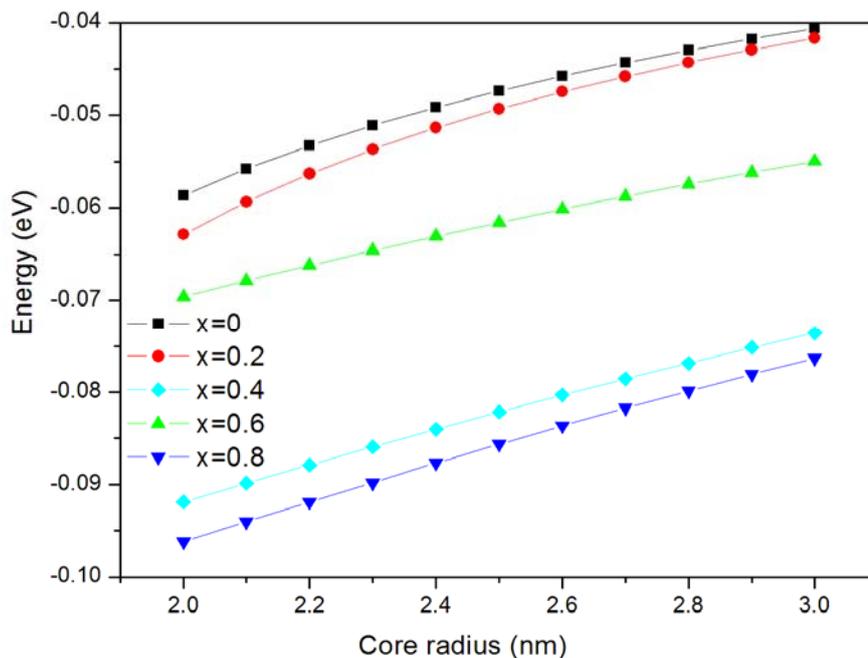
QDs structure with the different Se molar fraction.

Fig. 6 The Coulomb interaction energy as a function of the core radius in ZnTeSe/ZnSe

QDs structure with the different Se molar fraction.

Fig.6 reveals the Coulomb interaction energy of the ground state for the ternary $ZnTe_{1-x}Se_x/ZnSe$ core/shell as a function of the core radius for the five different Se molar fraction x=0, 0.2, 0.4, 0.6, and 0.8, respectively. The Coulomb interaction energy strongly depends on the core radius and the type of QDs. The strength of the Coulomb interaction energy decreases as the core radius is increased. According to the expression (5), the overlap integral play an important role in carrier-carrier interaction. Thus, the QDs with small size core, which results in a large overlap integral due to the strong confining of carriers. It can also been seen that the Coulomb interaction energy are stronger in the type-I QDs than that in the type-II QDs, which can results from large overlap integral in type-I QDs.

4. Conclusions

In general, we study the electronic structures of a ternary $ZnTe_{1-x}Se_x/ZnSe$ core/shell structure QDs, including the Coulomb interaction between electron and hole. It is found that the $1s$ transition energies depend sensitively on the core radius of the QDs and Se molar fraction in the ternary core. The spatial separation between electron and hole in QDs can easily be implemented by adjusting Se molar fraction in the core region. The heterostructure types of QDs can be classified as Type-I, quasi Type-II, and Type-II with changing of the Se molar composition in QDs, which can be ascribed to the bowing parameters in the ternary semiconductor compound. The Coulomb interaction energy are stronger in the type-I QDs than that in the type-II QDs, which can results from large overlap integral in type-I QDs.

Acknowledgements

References

[1] R. Najjar, Andre, R.; Besombes, L.; Bougerol, C.; Tatarenko, S.; Mariette, H., Materials Science and Engineering B-Advanced Functional Solid-State Materials, **165** (1-2), 85-87 (2009)
[2] Ivanov, S. A.; Piryatinski, A.; Nanda, J.; Tretiak, S.; Zavadil, K. R.; Wallace, W. O.; Werder, D.; Klimov, V. I., Journal of the American Chemical Society, **129** (38), 11708 (2007).
[3] Piryatinski, A.; Ivanov, S. A.; Tretiak, S.; Klimov, V. I., Nano Letters, **7**(1), 108 (2007).
[4] Kim, S.; Fisher, B.; Eisler, H. J.; Bawendi, M., Journal of the American Chemical Society, **125**(38), 11466 (2003).
[5] Haus, J. W.; Zhou, H. S.; Honma, I.; Komiyama, H., Physical Review B (Condensed Matter), **47** (3), 1359 (1993).
[6] Bang, J.; Park, J.; Lee, J. H.; Won, N.; Nam, J.; Lim, J.; Chang, B. Y.; Lee, H. J.; Chon, B.; Shin, J.; Park, J. B.; Choi, J. H.; Cho, K.; Park, S. M.; Joo, T.; Kim, S., Chemistry of Materials, **22**(1), 233 (2010).
[7] Chi-Che, T.; Shih-Yen, L.; Wei-Hsun, L.; Shu-Cheng, M.; Shung-Yi, W.; Shu-Han, C.; Jen-Inn, C., Room-temperature Operation Type-II GaSb/GaAs Quantum-dot Infrared Light-emitting Diode. 2010 22nd International Conference on Indium Phosphide and Related

Materials (IPRM 2010) 2010, 3 pp.

[8] Sierra-Ortega, J.; Escorcia, R. A.; Mikhailov, I. D., Exciton in type-II quantum dot. Journal of Physics: Conference Series 2009, 012034 (5 pp.).

[9] Bartnik, A. C.; Wise, F. W.; Kigel, A.; Lifshitz, E., Electronic structure of PbSe/PbS core-shell quantum dots. Physical Review B, 75 (24), 2007

[10] Oron, D.; Kazes, M.; Banin, U., Multiexcitons in type-II colloidal semiconductor quantum dots. Physical Review B, **75**(3), 7 (2007).

[11] Gomes, P. F.; de Godoy, M. P. F.; Dias, G. O.; Iikawa, F.; Brasil, M. J. S. P.; Cotta, M. A.; Journal of Physics D: Applied Physics, 045303 (5 pp.) 2010

[12] Lin, S. Y.; Tseng, C. C.; Lin, W. H.; Mai, S. C.; Wu, S. Y.; Chen, S. H.; Chyi, J. I., Applied Physics Letters, 96 (12) 2010.

[13] Zhang, W. H.; Yu, J. S., Chinese Journal of Inorganic Chemistry, **26**(5), 775 (2010).

[14] Gradkowski, K.; Pavarelli, N.; Ochalski, T. J.; Williams, D. P.; Tatebayashi, J.; Huyet, G.; O'Reilly, E. P.; Huffaker, D. L., Applied Physics Letters, 95 (6) 2009.

[15] Huyet, G.; Ochalski, T. J.; Williams, D. P.; Gradkowski, K.; O'Reilly, E. P.; Pavarelli, N.; Tatebayashi, J.; Huffaker, D. L., Applied Physics Letters 2009, 061102 (3 pp.).

[16] Nemchinov, A.; Kirsanova, M.; Hewa-Kasakarage, N. N.; Zamkov, M., Journal of Physical Chemistry C, **112** (25), 9301 (2008).

[17] Wang, C. H.; Chen, T. T.; Chen, Y. F.; Ho, M. L.; Lai, C. W.; Chou, P. T., Nanotechnology , 19 (11) 2008.

[18] Balet, L. P.; Ivanov, S. A.; Piryatinski, A.; Achermann, M.; Klimov, V. I., Nano Letters, **4**(8), 1485 (2004).

[19] He, J.; Reyner, C. J.; Liang, B. L.; Nunna, K.; Huffaker, D. L.; Pavarelli, N.; Gradkowski, K.; Ochalski, T. J.; Huyet, G.; Dorogan, V. G.; Mazur, Y. I.; Salamo, G. J., Nano Letters, **10**(8), 3052-3056 (2010).

[20] Gurusinghe, N. P.; Hewa-Kasakarage, N. N.; Zamkov, M., Journal of Physical Chemistry C **112** (33), 12795 (2008).

[21] Zhong, X. H.; Han, M. Y.; Dong, Z. L.; White, T. J.; Knoll, W., Journal of the American Chemical Society, **125**(28), 8589 (2003).

[22] Wang, Y.; Hou, Y. B.; Tang, A.; Feng, B.; Li, Y.; Liu, J.; Teng, F., Journal of Crystal Growth **308**, 19 (2007).

[23] Nizamoglu, S.; Demir, H. V., Optics Express, **16**(6), 3515 (2008).

[24] Schooss, D.; Mews, A.; Eychmuller, A.; Weller, H., Physical Review B (Condensed Matter), **49**(24), 17072 (1994).

[25] Chang, K.; Xia, J. B., Physical Review B, **57**(16), 9780-9786 (1998).

[26] Kamata, A.; Yoshida, H.; Chichibu, S.; Nakanishi, H., Journal of Crystal Growth, **170**(1-4), 518 (1997).

[27] Tit, N.; Obaidat, I. M.; Alawadhi, H., Journal of Physics-Condensed Matter, **21**(7), 6 (2009).

[28] Vanecek, M.; Klier, E., Physica Status Solidi A, **30** (2), 441 (1975).

[29] Bhunia, S.; Bose, D. N., Journal of Applied Physics, **87**(6), 2931-2935 (2000)